

Article

Wear Behaviour of A356/TiAl₃ *in Situ* Composites Produced by Mechanical Alloying

Seda Çam, Vedat Demir and Dursun Özyürek *

Manufacturing Engineering of Technology Faculty, Karabuk University, 78100 Karabuk, Turkey; msfe_0180@hotmail.com (S.C.); vdemir@karabuk.edu.tr (V.D.)

* Correspondence: dozyurek@karabuk.edu.tr; Tel.: +90-370-433-82-00; Fax: +90-370-433-82-04

Academic Editor: Sherif D. El Wakil

Received: 26 December 2015; Accepted: 2 February 2016; Published: 5 February 2016

Abstract: In this study, the effects of *in situ* TiAl₃ particles on dry sliding wear behavior of A356 aluminum alloy (added Ti) composites were investigated. The wear samples were prepared by adding different amounts of Ti (4%, 6%, and 8%) into A356 powder alloy by mechanical alloying. The mechanically alloyed powders were cold pressed at 600 MPa and sintered 530 °C for 1 h in argon atmosphere and cooled in the furnace. After the sintering process, the samples were characterized. The results show that AlTi and TiAl₃ intermetallic phases were formed and their amount increased depending on the amount of Ti added into A356 powder alloy. Out of the samples sintered with different titanium amounts (1 h at 530 °C), the highest hardness value and, accordingly, the lowest wear amount, were observed in the alloy containing 8% Ti.

Keywords: A356-Ti alloys; mechanical alloying; sintering; wear behavior

1. Introduction

Aluminum and its alloys are commonly used in structural applications in the automotive and aerospace industry, owing to their low densities and high specific resistances. However, these materials have poor tribological properties [1]. Magnesium is an important element which forms a significant solid solution in Al-Si alloys and increases the strengths of alloys with precipitation hardening. A356 alloys constitute the most important group of Al-Si-Mg alloys whose strength can be increased with Mg₂Si precipitates in Al matrix [2–5]. Another important method used to improve the mechanical properties of the alloy is to compose stable *in situ* intermetallic phases in the structure [6–8]. In the production of aluminum metal matrix composites (AMMC), which are defined as materials having superior tribological properties, the most common materials used as reinforcement phase are SiC [9–14], Al₂O₃ [15,16], TiB₂ [17,18] and TiC [19]. In the production of many AMMC materials, *ex situ* techniques are preferred (supplements made to the matrix *ex situ* in order to increase strength). The biggest contribution of *ex situ* addition of reinforcement materials to the matrix is that they protect the stable condition of the reinforcement phase in the structure at elevated temperatures. However, certain reinforcement phases are subject to phase transformation at elevated temperatures and, thus, AMMCs exhibit unstable structure. As to *in situ* composite materials, reinforcement phases are formed during solidification, sintering, or synthesizing [7,20–22]. Thus, *in situ* reinforcement phases make processes shorter and reduce the costs. In Al-Ti alloy system, TiAl₃ and AlTi intermetallic phases are formed *in situ* at the equilibrium conditions and these phases increase the hardness and strength of AMMC materials. Aluminum alloys reinforced with aluminates particles are preferred due to their high strengths and mechanical properties at elevated temperatures [23,24]. In comparison to other Al-rich (NiAl₃, FeAl₃, etc.) intermetallic, they are more attractive as they have lower densities (3.4 gr/cm³) and higher melting points (~1350 °C) [22,25–27]. This present study aims at developing new materials

with improved wear properties by adding Ti to A356 alloy. The influence of intermetallic phases (TiAl₃ and AlTi) formed *in situ* during the sintering process on the wear behaviors were investigated.

2. Experimental Procedure

For the experimental studies, A356 (Al-Si-Mg) alloy powder having a mean particle size of <50 μm was used as the matrix material. The chemical composition of the alloy powder is given in Table 1. Titanium powder with 99.7% purity and 10 μm mean particle size was added into A356 alloy powder samples with three different percentages, namely 4%, 6%, and 8%, by weight. The samples were then mechanically alloyed for 45 min at 10:1 ball-to-powder ratio a SPEX SamplePreb unit (SPEX SamplePreb, Standmore, UK) [28]. The mechanically-alloyed A356-Ti powder samples were then cold pressed unidirectionally at 600 MPa to obtain 6 mm height small cylindrical samples having 10 mm diameter. The samples were sintered at 530 °C for 1 h at a 10 °C/min heating rate in an argon atmosphere and cooled in the furnace. After the sintering process had been completed, the samples were cleaned with alcohol and acetone and left to dry. Following standard metallographic processes, the samples were etched for 30–45 s with 2 mL (HF), 90 mL pure water, 5 mL (HNO₃), and 3 mL (HCl) for microstructural examinations. Archimedes' method was used for density measurements of the samples. Following the density measurements, the samples were characterized through X-ray diffraction method (XRD), scanning electron microscope (SEM) (FEI, Hilliboro, OR, USA), transmission electron microscope (TEM) (FEI, Hilliboro, OR, USA), and hardness measurements. For XRD examinations, an INEL unit (INEL, Artenay, France) was used, while a FEI Quanta 250 (30 kV) (FEI, Hilliboro, OR, USA) was used for SEM and EDS examinations. As for TEM examinations, an FEI Tecnai G2 F30 unit (200 kV) (FEI, Hilliboro, OR, USA) was used. Hardness values of the samples were determined by calculating the mean of five measurements obtained using an AFFRI hardness measurement device (HV2) (AFFRI, Olona, Italy). Wear tests were carried out on an AISI 4423 steel disc having 58 HRC and rotating continuously in a pin-on-disc wear device.

Table 1. Chemical composition of the A356 alloy.

Alloy	Si	Fe	Cu	Mn	Mg	Zn	Ti	Pb
A356	6.5	0.15	0.03	0.03	0.4	0.05	0.2	0.03

Prior to the wear tests, the surfaces of each sample were prepared with 1200 grade SiC abrasive to ensure a full contact between the abrasive steel disc and sample surfaces. All wear tests were carried out at room temperature and under dry sliding conditions. In these tests, a 30 N load, 1 m·s⁻¹ sliding speed, and five different sliding distances, namely 400 m, 800 m, 1200 m, 1600 m, and 2000 m, were used. Following the wear tests, the worn surfaces of the samples were examined using SEM.

3. Results and Discussion

Figure 1 gives SEM images of the microstructure of A356-Ti alloy sintered at 530 °C for 1 h. It is clear in Figure 1 that Ti added into a A356 matrix at different ratios (4%, 6%, and 8%) showed different distribution patterns in the microstructure following the mechanical alloying process. The presence of large titanium grains within the A356 matrix may be explained in two different ways. First, since the size of the titanium particles added into the matrix was too small (10 μm), the powders might have become agglomerated. Secondly, this situation may have resulted from the characteristic feature of the mechanical alloying process. As is well known, mechanical alloying is a solid-state process that starts with cold welding of powder particles that are squeezed between two balls and/or between a ball and the container wall, as high-energy balls crash into one another and the container wall during the process. Then, powder particles undergo work hardening and in the last phase, particles are fragmented. Previous studies reported a slight increase in the powder dimension with the effect of cold welding taking place in the first stage of the mechanical alloying process [29–31]. Therefore, titanium

powder particles in the matrix can be combined together during mechanical alloying and form coarse grains. Intermetallic compounds (TiAl_3), resulting from the reaction between Al matrix and Ti during sintering of cold-formed compacts, are also observed in the SEM images. It can also be seen that TiAl_3 intermetallic phase (Figure 1a) that seems to come out in the structure during sintering is surrounded by the matrix and is very small. In addition, a reaction takes place between the aluminum matrix and reinforcement phase interface in A356 alloy that has added titanium. This was also pointed out in a study carried out by Yu *et al.* [32].

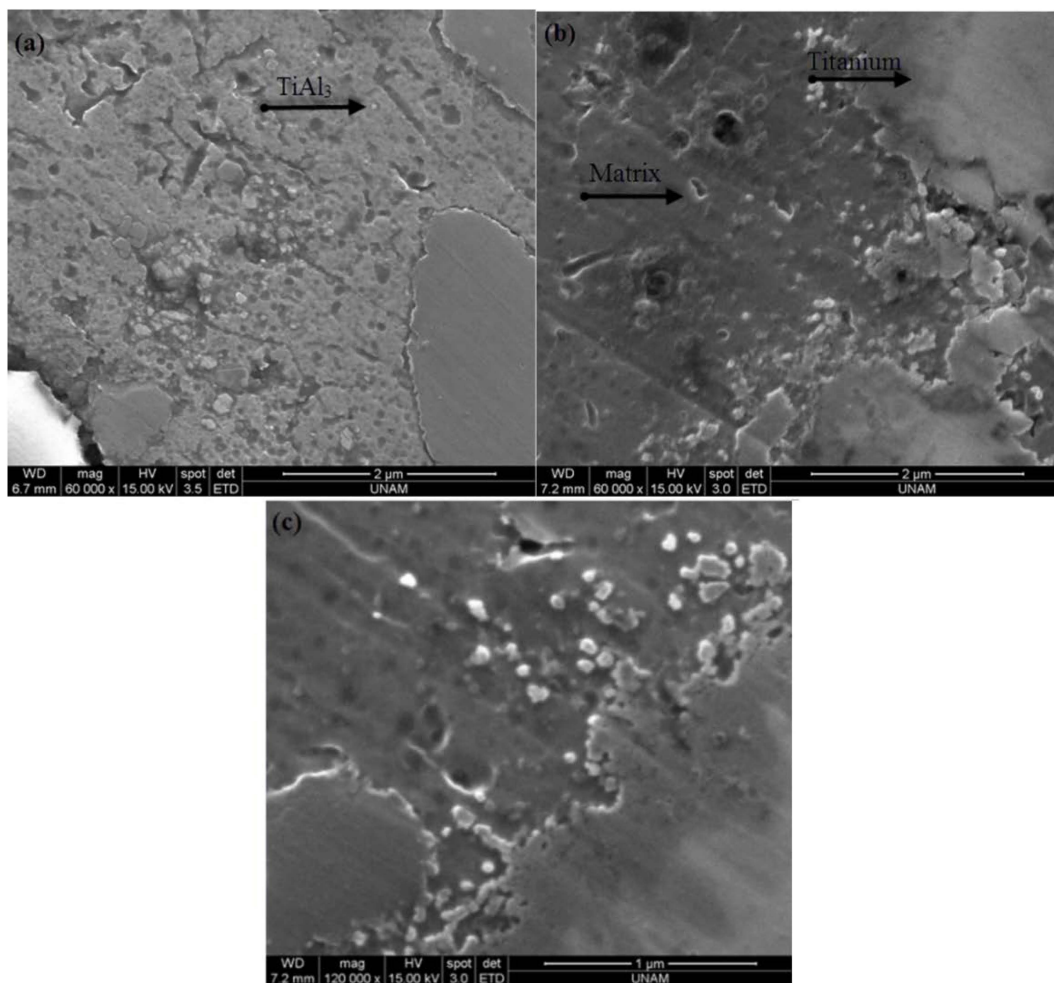


Figure 1. SEM images of Al-Ti alloys 4% Ti (a); 6% Ti (b); and 8% Ti (c) sintered at 530 °C for 1 h.

AlTi and TiAl_3 particles are formed *in situ* form within the matrix [8,33]. To better examine the dimensions of intermetallic compounds formed in the *in situ* structure, TEM examinations were carried out. Figure 2 gives an image of TEM bright-area and selected-area diffraction pattern, where it is seen that *in situ* titanium aluminate particles with a particle size of about 50 nm are formed in the structure during the sintering.

In the bright-area TEM image, TiAl_3 intermetallic phase is evident in A356 matrix depending on the sintering process. Additionally, a ringed structure is clearly seen in the diffraction pattern image of the selected area. The ringed appearance is associated with deformation of the crystal structure during the mechanical alloying process as well as the formation of a harmonic, wide-angle grain structure. An increase in the amount of deformation occurring in the powder particles during the mechanical alloying process reduces the recrystallization temperature. Thus, a larger grained structure is expected to form during the sintering following the deformation. However, as Ti is added into the A356 matrix it

reacts and forms a TiAl_3 phase, it is clear that the grain growth of newly-formed grains in the structure is not excessive. This is because of the fact that certain phases added into the Al matrix, such as TiAl_3 , TiB_2 , TiC , and B, inhibit the grain growth [17,34]. X-ray diffraction results of A356-Ti alloy having different ratios of Ti are given in Figure 3.

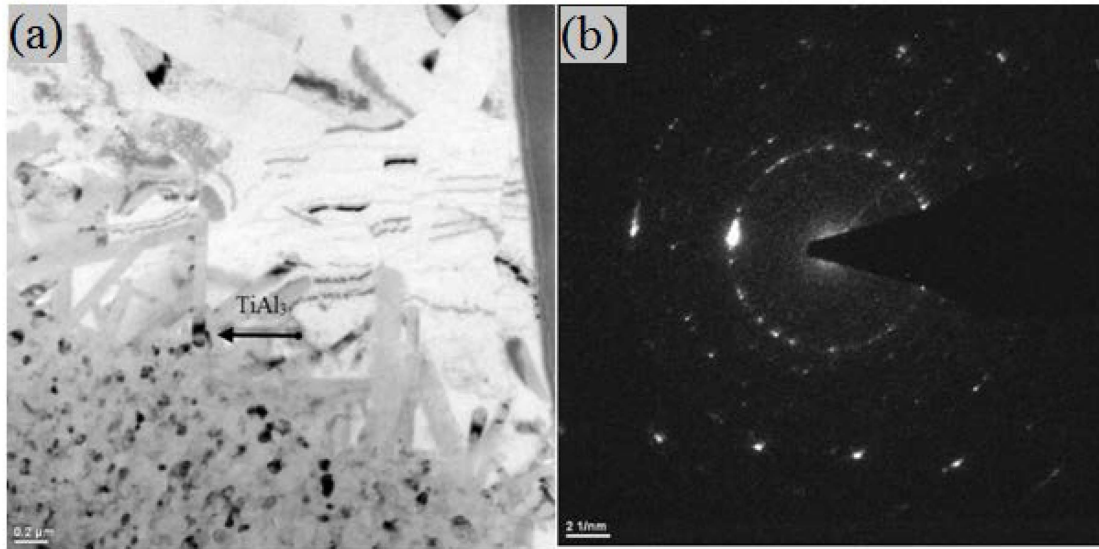


Figure 2. TEM images of 6% Ti added A356 alloy bright-area (a) and selected-area (b) diffraction pattern.

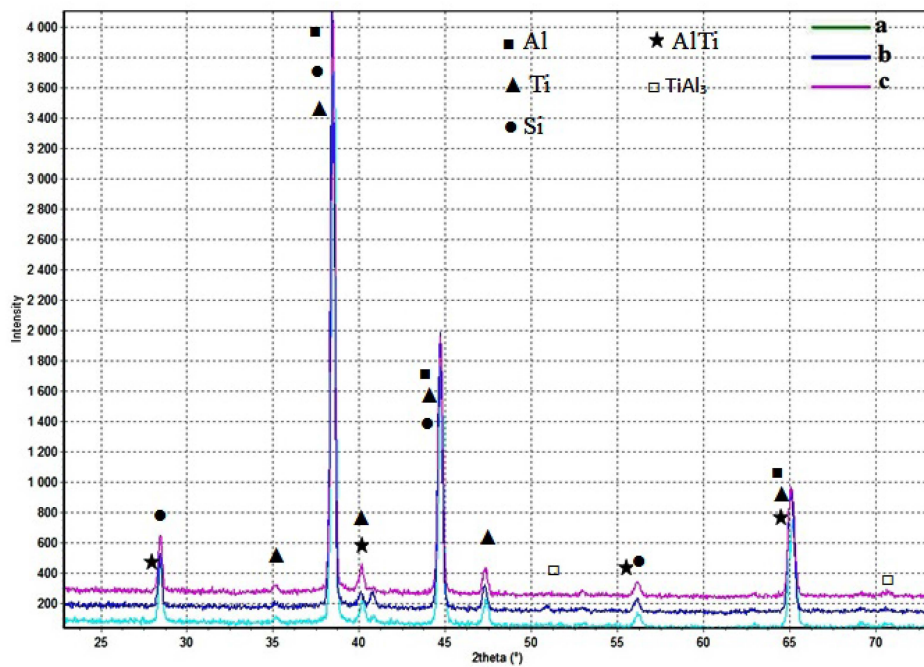


Figure 3. XRD results of A356-Ti alloy with 4% (a); 6% (b); and 8% (c) Ti.

It is known that different intermetallic compounds (α_2 - Ti_3Al , γ - TiAl , TiAl_3 , and TiAl_2) are formed in the Al-Ti phase diagram depending on the ratios of Al and Ti elements and alloying conditions [35]. In the present study, it was determined that TiAl_3 and AlTi reinforcement phases which were expected to be formed in the structure with X-ray diffraction were actually formed via *in situ* reactions. This *in situ* reaction is as follows:



In situ titanium aluminate intermetallic compounds in the structure are intermetallic compounds whose crystal structures are different from metals. In the study conducted by Chianeh *et al.* [33], it was reported that only the TiAl_3 intermetallic phase was obtained in the samples sintered at $500\text{ }^\circ\text{C}$ for 9 h and the samples sintered at $600\text{ }^\circ\text{C}$ for 3 h. In this study, XRD results given in Figure 3 show that both AlTi and TiAl_3 phases can be formed following sintering at $530\text{ }^\circ\text{C}$ for 1 h. XRD results also demonstrate that the TiAl_3 phase can be formed during the sintering lasting for 1 h and increases depending on the increase in the Ti amount added into the alloy. Post-sintering hardness values of A356-Ti powder alloy produced with mechanical alloying where different amounts of Ti are added are given in Figure 4.

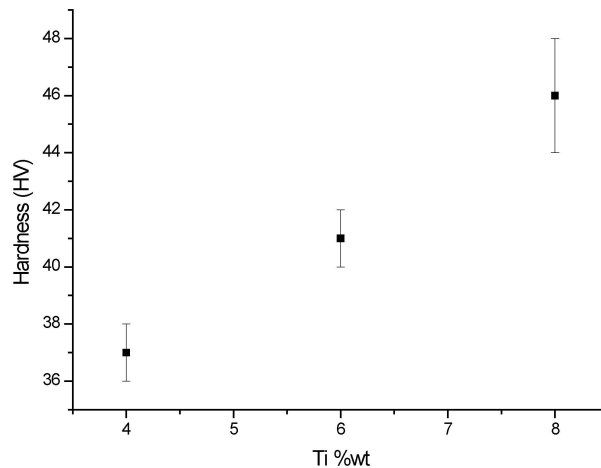


Figure 4. Hardness values of A356 different amounts of Ti added.

As can be seen in Figure 4, the hardness values of samples containing 4% Ti, 6% Ti, and 8% Ti are 37 HV, 41 HV, and 46 HV, respectively. The lowest hardness value was observed for the samples containing 4% Ti, while the highest hardness value was measured for the samples containing 8% Ti. Accordingly, as the Ti amount in the alloy increases, the hardness of Al-Ti alloy also increases. That increase in hardness is associated with the increase of the volume fraction of the TiAl_3 intermetallic phase. This finding is supported by a previous study [8]. Post-sintering densities of A356 alloy into which different amounts of Ti were added are given in Figure 5. Archimedes method was used for the density measurement.

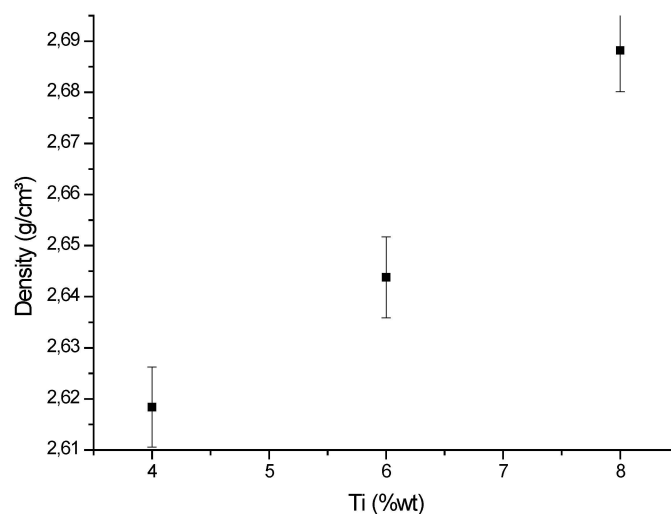


Figure 5. Densities of A356 alloy containing different amounts of Ti.

When post-sintering density values of A356 alloy into which different amounts of Ti were added are examined, the highest value is observed for the samples containing 8% Ti ($2.68 \text{ g}\cdot\text{cm}^{-3}$), while the lowest value is obtained for the samples containing 4% Ti ($2.61 \text{ g}\cdot\text{cm}^{-3}$). As the amount of % Ti in the alloy increases, density and hardness values of alloys also increase. The reason behind this hardness and density increase is the fact that the density of titanium is higher than the density of A356 alloy. Weight losses of A356-Ti alloys produced with mechanical alloying under 30 N load for different distances (400 m, 800 m, 1200 m, 1600 m, and 2000 m) are given in Figure 6.

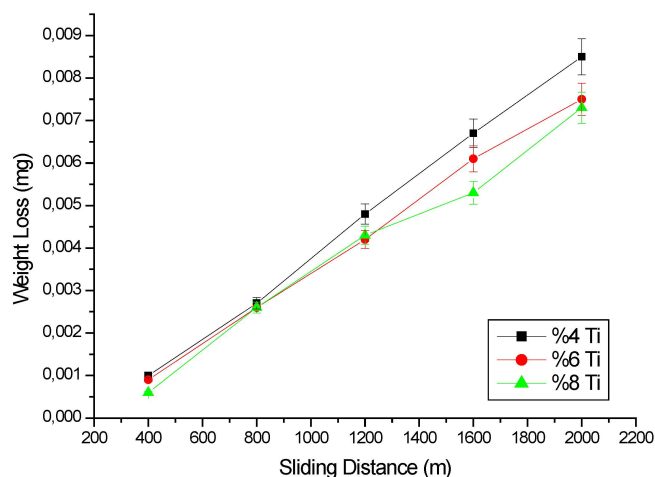


Figure 6. Weight losses of the samples depending on the sliding distances.

As evident in Figure 6, the highest weight loss occurs in the alloy containing 4% Ti, while the lowest weight loss is observed for the alloy containing 8% Ti. However, weight loss values of the alloys containing 6% and 8% Ti are extremely close to each other. The highest weight loss of the sample containing 4% Ti can be attributed to its lower hardness, as well as the lower amount of intermetallic phases. The hardness of the AMCs increased with increasing Ti amount. As it is known, the weight loss of a material in a wear test decreases with an increase in the hardness of the material [12,15]. Venci *et al.* [36] pointed out that the rate of reinforcement should be increased to reduce plastic deformation and to increase hardness of the material. Average friction coefficients of Al-Ti alloys containing different amounts of titanium (at the end of 2000 m) are given in Figure 7.

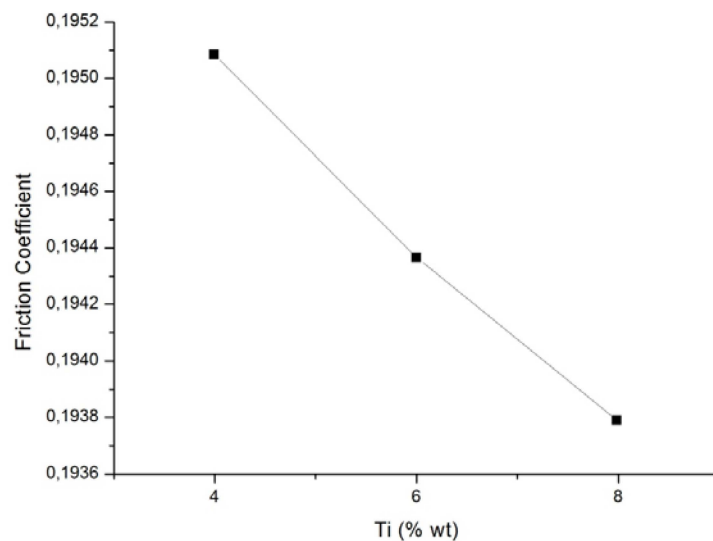


Figure 7. Average friction coefficients of Al-Ti alloys.

The friction coefficients given in the Figure 7 are average values obtained for each alloy at the end of 2000 m sliding distance. The lowest friction coefficient was obtained for the alloy containing 8% Ti, while the highest friction coefficient was obtained for the alloy containing 4% Ti. As there is a relationship between weight losses and friction coefficients, the friction coefficient decreases with the increase in the hardness of the alloy. It was determined that both the weight loss and friction coefficient of the alloy, which has the lowest hardness value and contains 4% Ti are higher than the others. SEM images taken from the worn surfaces of Al-Ti alloys are given in the Figure 8.

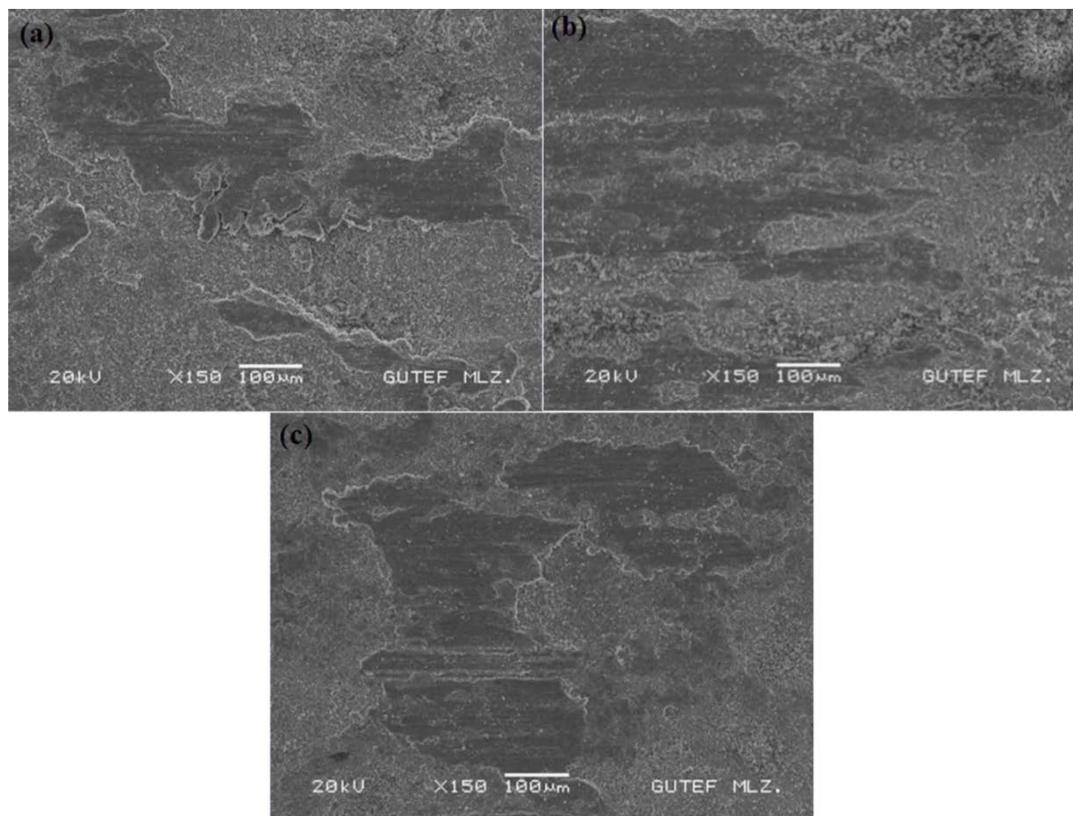


Figure 8. SEM images of the worn surface of Al-Ti alloys 4% Ti (a); 6% Ti (b); and 8% Ti (c).

When the SEM image of the worn surface of Al-4% Ti alloy that has the highest weight loss is examined (Figure 8a), it is seen that plastic deformation and adhesion occurred on the surface. That can be explained by the fact that the particles pulled off the surface during the wear test are moved and smeared onto the worn surface once more [37,38]. Smearing which occurs during the wear test is also observed in the worn surfaces of other alloys containing 6% Ti and 8% Ti. Another important point observed from the worn surfaces is the lack of deep marks on the surface. Additionally, it is seen that oxidation occurs on the worn surfaces of the samples into which 4%, 6%, and 8% titanium are added. As mentioned in a previous study, the oxidation on the worn surfaces results from the heat caused by the friction occurring during the wear tests [18]. That stable oxide structure forming on the worn surfaces acts as solid lubricant during dry sliding. When looking at the hardness values in Figure 4, it is clear that as the amount of titanium added into the alloy increases, hardness also increases. Another impact of hardness values (Figure 7) is that friction coefficients decrease depending on the titanium amount added into the alloy.

4. Conclusions

In the present study, Al-Ti alloy powders were produced by mechanical alloying to contain 4%, 6% and 8% titanium respectively. They were then compacted cold and sintered at 530 °C for 1 h. The effect

of the percentage of titanium on the hardness and the wear properties of the various sintered samples were examined. The following could be concluded:

- As the amount of Ti in Al-Ti alloys increases, the hardness value increases.
- As the amount of added Ti increases in the composites, the density value also increases since the density of Ti is higher than that of Al.
- The XRD examinations show that the titanium aluminate phases (TiAl_3 and AlTi), which increase strength in the samples, are formed in the alloy following the sintering process.
- The amount of intermetallic phases in the structure during sintering increases depending on the increasing titanium addition and that affects the wear properties.
- Sintered samples with higher percentages of titanium would exhibit less weight loss and a lower coefficient of friction.

Author Contributions: Study design: D. Özyürek and V. Demir; Experimental work: S. Cam; Results analysis and Manuscript preparation: All authors; Manuscript proof and submission: D. Özyürek.

Conflicts of Interest: The authors declare no conflict of interest.

References

1. Kumar, S.; Balasubramanian, V. Developing a mathematical model to evaluate wear rate of AA7075/SiC_p powder metallurgy. *Wear* **1999**, *264*, 1026–1034. [[CrossRef](#)]
2. Azadi, M.; Shirazabad, M.M. Heat treatment effect on thermo-mechanical fatigue and low cycle fatigue behaviors of A356.0 aluminum alloy. *Mater. Des.* **2013**, *45*, 279–285. [[CrossRef](#)]
3. Ragab, K.A.; Samuel, A.M.; Al-Ahmari, A.M.A.; Samuel, F.H.; Doty, H.W. Influence of fluidized sand bed heat treatment on the performance of Al-Si cast alloys. *Mater. Des.* **2011**, *32*, 1177–1193. [[CrossRef](#)]
4. Zhu, M.; Jian, Z.; Yang, G.; Zhou, Y. Effects of T6 heat treatment on the microstructure, tensile properties and fracture behavior of the modified A356 alloys. *Mater. Des.* **2012**, *36*, 243–249. [[CrossRef](#)]
5. Kliauga, A.M.; Vieira, E.A.; Ferrante, M. The influence of impurity level and tin addition on the aging heat treatment of the 356 class alloy. *Mater. Sci. Eng. A* **2008**, *480*, 5–16. [[CrossRef](#)]
6. Ahmed, S.; Haseeb, A.S.M.A.; Kurny, A.S.W. Study of wear behaviour of Al-4.5% Cu-3.4% Fe *in situ* composite: Effect of thermal and mechanical processing. *J. Mater. Process. Tech.* **2007**, *182*, 327–332. [[CrossRef](#)]
7. Niu, L.; Zhang, J.; Yang, X. *In-situ* synthesis of Al₃Ti particles reinforced Al-Based composite coating. *Trans. Nonferrous Met. Soc. China* **2012**, *22*, 1387–1393. [[CrossRef](#)]
8. Özyürek, D.; Tekeli, S.; Tuncay, T.; Yılmaz, R. The effect of synthesis time on the wear behavior of Al-8% Ti alloy produced by mechanical alloying. *Powder Metall. Met. Ceram.* **2012**, *51*, 491–495.
9. Lu, L.; Lai, M.O.; Ng, C.W. Enhanced mechanical properties of an Al based metal matrix composite prepared using mechanical alloying. *Mater. Sci. Eng. A* **1998**, *252*, 203–211. [[CrossRef](#)]
10. Hu, Q.; McColl, I.R.; Harris, S.J.; Waterhouse, R.B. The role of debris in the fretting wear of a SiC reinforced aluminium alloy matrix composite. *Wear* **2000**, *245*, 10–21. [[CrossRef](#)]
11. Zhao, N.; Nash, P.; Yang, X. The effect of mechanical alloying on SiC distribution and the properties of 6061 aluminum composite. *J. Mater. Process. Tech.* **2005**, *170*, 586–592. [[CrossRef](#)]
12. Özyürek, D.; Tekeli, S. An investigation on wear resistance of SiC_p-reinforced aluminium composites produced by mechanical alloying. *Sci. Eng. Compos. Mater.* **2010**, *17*, 31–38. [[CrossRef](#)]
13. Aztekin, H.; Özyürek, D.; Çetinkaya, K. Production of hypo-eutectic Al-Si alloy based metal matrix composite with thixomoulding processing. *High Temp. Mater. Process.* **2010**, *29*, 169–178. [[CrossRef](#)]
14. Walker, J.C.; Rainforth, W.M.; Jones, H. Lubricated sliding wear behaviour of aluminium alloy composites. *Wear* **2005**, *259*, 577–589. [[CrossRef](#)]
15. Özyürek, D.; Tekeli, S.; Güral, A.; Meyveci, A.; Gürü, M. Effect of Al₂O₃ amount on microstructure and wear properties of Al-Al₂O₃ metal matrix composites prepared using mechanical alloying method. *Powder Metall. Met. Ceram.* **2010**, *49*, 289–294. [[CrossRef](#)]
16. Daoud, A.; Reif, W. Influence of Al₂O₃ particulate on the aging response of A356 Al-based composites. *J. Mater. Process. Tech.* **2002**, *123*, 313–318. [[CrossRef](#)]

17. Mandal, A.; Murty, B.S.; Chakraborty, M. Wear behaviour of near eutectic Al-Si alloy reinforced with *in-situ* TiB₂ particles. *Mater. Sci. Eng. A* **2009**, *506*, 27–33. [[CrossRef](#)]
18. Özyürek, D.; Ciftci, I. An investigation into wear behaviour of TiB₂ particle reinforced aluminum composites produced by mechanical alloying. *Sci. Eng. Compos. Mater.* **2011**, *18*, 5–12. [[CrossRef](#)]
19. Ruiz-Navas, E.M.; Fogognolo, J.B.; Valesco, J.B.; Ruiz-Prieto, J.M.; Froyen, L. One step production of aluminium matrix composite powders by mechanical alloying. *Compos. A Appl. Sci. Manuf.* **2006**, *37*, 2114–2120. [[CrossRef](#)]
20. Clemens, H.; Wallgram, W.; Kremmer, S.; Ther, V.G.; Otto, A.; Bartels, A. Design of novel β -solidifying TiAl alloys with adjustable β /B2-phase fraction and excellent hot-workability. *Adv. Eng. Mater.* **2008**, *10*, 707–713. [[CrossRef](#)]
21. Tetsui, T.; Shindo, K.; Kaji, S.; Kobayashi, S.; Takeyama, M. Fabrication of TiAl components by means of hot forging and machining. *Intermetallics* **2005**, *13*, 971–978. [[CrossRef](#)]
22. Hsu, C.J.; Chang, C.Y.; Kao, P.W.; Ho, N.J.; Chang, C.P. Al-Al₃Ti noncomposites produced *in-situ* by friction stir processing. *Acta Mater.* **2006**, *54*, 5241–5249. [[CrossRef](#)]
23. Yeh, C.L.; Su, S.H. *In situ* formation of TiAl-TiB₂ composite by SHS. *J. Alloy. Compd.* **2006**, *407*, 150–156. [[CrossRef](#)]
24. Liu, Y.; Xiu, Z.; Wu, G.; Jiang, L.; Gou, H.; Jiang, G. Microstructure evolution of Ti-Al-C system composite. *Rare Met. Mater. Eng.* **2010**, *39*, 1152–1156.
25. Shi, T.; Zhang, J.; Wang, L.; Jiang, W.; Chen, L. Fabrication, microstructure and mechanical properties of TiC/Ti₂AlC/TiAl₃ *in situ* composite. *J. Mater. Process. Tech.* **2011**, *27*, 239–244.
26. Wang, T.; Zhang, J. Thermoanalytical and metallographical investigations on the synthesis of TiAl₃ from elementary powders. *Mater. Chem. Phys.* **2006**, *99*, 20–25. [[CrossRef](#)]
27. Prakash, U.; Sauthoff, G. Structure and properties of Fe-Al-Ti intermetallic alloys. *Intermetallics* **2001**, *9*, 107–112. [[CrossRef](#)]
28. Özyürek, D.; Tunçay, T.; Evlen, H.; Çiftçi, I. Synthesis, Characterization and Dry Sliding Wear Behavior of *In-situ* Formed TiAl₃ Precipitate Reinforced A356 Alloy Produced by Mechanical Alloying Method. *Mater. Res.* **2015**, *18*, 813–820.
29. Rafiei, M.; Khademzadeh, S.; Parvin, N. Characterization and formation mechanism of nanocrystalline W-Al alloy prepared by mechanical alloying. *J. Alloy. Compd.* **2010**, *489*, 224–227. [[CrossRef](#)]
30. Tang, H.; Cheng, Z.; Liu, J.; Ma, X. Preparation of a high strength Al-Cu-Mg alloy by mechanical alloying and press-forming. *Mater. Sci. Eng. A* **2012**, *550*, 51–54. [[CrossRef](#)]
31. Gu, D.; Zhang, G.; Dai, D.; Wang, H.; Shen, Y. Nanocrystalline tungsten-nickel heavy alloy reinforced by *in-situ* tungsten carbide: Mechanical alloying preparation and microstructural evolution. *Int. J. Refract. Met. Hard Mater.* **2013**, *37*, 45–51. [[CrossRef](#)]
32. Yu, P.; Zhang, L.C.; Zhang, W.Y.; Das, J.; Kim, K.B.; Eckert, J. Interfacial reaction during the fabrication of Ni60Nb40 metallic glass particles-reinforced Al based MMCs. *Mater. Sci. Eng. A* **2007**, *444*, 206–213. [[CrossRef](#)]
33. Chianeh, V.A.; Hossein, H.R.; Nofar, M. Microstructural features and mechanical properties of Al-Al₃Ti composite fabricated by *in-situ* powder metallurgy route. *J. Alloy. Compd.* **2009**, *473*, 127–132. [[CrossRef](#)]
34. Rao, A.K.P.; Das, K.; Murty, B.S.; Chakraborty, M. Microstructural and wear behavior of hypoeutectic Al-Si alloy (LM25) grain refined and modified with Al-Ti-C-Sr master alloy. *Wear* **2006**, *261*, 133–139.
35. Mishin, Y.; Herzig, C. Diffusion in the Ti-Al system. *Acta Mater.* **2000**, *48*, 589–623. [[CrossRef](#)]
36. Vencel, A.; Rac, A.; Bobic, I.; Miskovic, Z. Tribological properties of Al-Si alloy reinforced with Al₂O₃ particles. *Tribol. Ind.* **2006**, *28*, 27–31.
37. Sağlam, I.; Özyürek, D.; Çetinkaya, K. Effect of ageing treatment on wear properties and electrical conductivity of Cu-Cr-Zr alloy. *Bull. Mater. Sci.* **2011**, *34*, 1465–1470. [[CrossRef](#)]
38. Attar, H.; Prashanth, K.G.; Chaubey, A.K.; Calin, M.; Zhang, L.C.; Scudino, S.; Eckert, J. Comparison of wear properties of commercially pure titanium prepared by selective laser melting and casting processes. *Mater. Lett.* **2015**, *142*, 38–41. [[CrossRef](#)]

